DNS OF AEROSOL EVOLUTION IN A TURBULENT MIXING LAYER

K. Zhou, A. Attili, A. Alshaarawi, and F. Bisetti
Clean Combustion Research Center
King Abdullah University of Science and Technology
Thuwal 23955, Kingdom of Saudi Arabia
E-mail: kun.zhou@kaust.edu.sa (K. Zhou)

ABSTRACT

The complex interaction of turbulent mixing and aerosol growth processes in a canonical turbulent flow configuration is investigated by means of direct numerical simulation. A cold gaseous stream mixes with a hot stream of vapor in a developing mixing layer. Nanometer sized particles (droplets) nucleate as vapor becomes supersaturated and subsequently grow as more vapor condenses on their surface. Aerosol dynamics are solved with the Quadrature Method of Moments. Aerosol moments advection is solved with a Lagrangian particles scheme. The results show that the highest nucleation rate region is located on the cold, lean vapor region, while particles experience a high growth rate on the hot, rich vapor region. The effect of differential diffusion of aerosol particles and the gas is investigated. Small nucleated particles tend to drift towards the hot, rich vapor region, while bigger particles drift towards the cold, lean vapor region, and the particle volume fraction peaks in the middle region of the mixture fraction space. Monte Carlo simulation of aerosol evolution is perfomred along a selected Lagrangian trajectory to analyze the particle size distribution, which is found to exhibits complex modality due to the synergistic effect of nucleation and condensation.

INTRODUCTION

Aerosols are ubiquitous both in nature and in industrial products, for example, clouds, air pollution such as smog and smoke, soot in flames, cement dust etc. Aerosol dynamics generally involve three fundamental processes: nucleation, condensation, and coagulation. Aerosol particles evolution is extremely sensitive to the history of temperature and vapor concentration that these particles undergo. Therefore it is very difficult to investigate the complex interaction between turbulence mixing and aerosol growth processes.

In their seminal work, Lesniewski & Friedlander (1998) measured dibutyl phthalate (DBP) particle nucleation and growth in a free turbulent jet. Since then, a few numerical simulations have been done to investigate aerosol particles formation and growth in turbulent jets. Garmory & Mastorakos (2008) and Veroli & Rigopoulos (2011) simulated DBP aerosol evolution in the turbulent jet flow same as the experimental configuration of Lesniewski & Friedlander (1998). In the simulation of Garmory & Mastorakos (2008), Reynold's stress model for turbulence was used, combined with the stochastic fields transported probability density function (pdf) method to model aerosol evolution. Veroli & Rigopoulos (2011) developed the trans-

ported population balance equation-pdf approach, based on a $k - \varepsilon$ model for turbulence. Garmory & Mastorakos (2008) and Veroli & Rigopoulos (2011) found discrepancies during comparing their simulation results with the measurements of Lesniewski & Friedlander (1998), and attributed those discrepancies to the inability of the numerical methods to correctly model the coupling between turbulence and aerosol dynamics, and the uncertainty in the aerosol kinetics and the experimental procedure.

In this study, Direct Numerical Simultion (DNS) combined with the Quadrature Method of Moments (QMOM) (McGraw, 1997; Marchisio *et al.*, 2003) is used to simulate DBP aerosol evolution in a turbulent mixing layer. A Lagrangian particles scheme (Attili & Bisetti, 2013) is used to convect the moments set. The purpose of this simulation is twofold. First, DNS provides a way to "generate" the canonical turbulent mixing layer with high fidelity (Attili & Bisetti, 2012). The effects of turbulence on aerosol formation and growth can be studies without resorting to empirical turbulence models and various closure models when coupling the GDE with turbulence models. Second, combing the Lagrangian particles scheme with a method of moments works as a prototype for simulations of aerosol evolution in turbulence. Along a selected Lagrangian trajectories, a Monte Carlo (MC) is used to simulate the aerosol evolution, which gives the aerosol particle size distribution (psd) that is not available in a method of moments.

MODELS AND EQUATIONS
Fluid dynamics

The DNS presented here is performed by solving the incompressible Navier-Stokes equations. The parallel flow solver "NGA" (Desjardins *et al.*, 2008) developed at Stanford University is used to solve the transport equations. The solver implements a finite difference method on a spatially and temporally staggered grid with the semi-implicit fractional step method of Kim & Moin (1985). Velocity is discretized with a second order finite differences centered scheme. The time step size is calculated to guarantee the maximum Courant-Friedrichs-Lewy number over the field to be smaller than 0.8. A pressure-correction step involving the solution of a Poisson equation ensures mass conservation. The code decomposes the computational domain over a number of processors and implements a distributed memory parallelization strategy using the message passing interface. The solution of the Poisson equation on massively parallel machines is performed by the library HYPRE (Falgout *et al.*, 2006) using the preconditioned conjugate gra-

dient iterative solver coupled with one iteration of an algebraic multigrid preconditioner.

At the inlet, velocity is imposed by combining two laminar boundary layers. The free convective outflow (Ol'shanskii & Staroverov, 2000) condition is used at the outlet. The boundary conditions are periodic in the spanwise direction z and free slip in the crosswise direction y. The free slip condition is applied by imposing a zero crosswise velocity component at the boundary. The normal derivatives of the streamwise and spanwise velocity components are set to zero.

The two streams have velocity $u_1 = 15$ and $u_2 = 5$ m/s. Random velocity fluctuation $0.4(\omega_t - 1)u$, where ω_t is a random variable from the standard uniform distribution, is superimposed on the velocity profile, resulting in the onset of Kelvin-Helmholtz instability in a very short distance downstream of the inlet. The computational domain is discretized with $768 \times 398 \times 256$ (80 million grid points), uniform in the region of interest. A posteriori analysis shows that the size of the grid is smaller than three times of the Kolmogorov scale

Temperature T and vapor mass fraction Y are assumed to be passive scalars, and are simulated by solving the convection-diffusion equation using the third order WENO scheme (Liu *et al.*, 1994). The effect of aerosol dynamics on the temperature field is neglected (e.g., latent heat of condensation), since the vapor mass fraction is very low (maximum 5000 ppm here). For vapor concentration, the consumption owing to gas-to-particle conversion is taken into account, i.e.,

$$\frac{\partial Y}{\partial t} + \nabla \cdot (\vec{u}Y) = D\nabla^2 Y + S_{\text{Aerosol}} \tag{1}$$

where $\vec{u}$ is the gas flow velocity, D is the diffusion coefficient, and the source term S_{Aerosol} denotes the vapor consumption due to gas-to-particle conversion. In the simulation, the Lewis number is assumed to be one, i.e., thermal diffusivity and mass diffusivity have the same value. The Schmidt number (ratio between kinematic viscosity and mass diffusivity) is also set to one. At the inlet, a hyperbolic tangent profile is used for the temperature with $T_{\text{max}} = 400$ and $T_{\text{min}} = 300$ K at the fast and slow streams, respectively. Similarly the profile for the vapor mass concentration is imposed with $Y_{\text{max}} = 5000$ and $Y_{\text{min}} = 0$ ppm.

The simulation was performed on the IBM Blue Gene/P supercomputer, "Shaheen", available at King Abdullah University of Science and Technology, using more than a million CPU hours. The total simulation time (after a statistically steady state is reached) is 2τ, where τ corresponds to the time during which the low-speed steam passes the whole domain. All mean statistics in this paper are obtained by averaging over different time instants and the periodic z (spanwise) direction, with around 10^4 samples. Figure 1 shows a snapshot of the simulated temperature field, which provides a schematic view of the simulation configuration.

Aerosol dynamics

In this work, all aerosol particles (droplets) are assumed to be spherical, characterized by the diameter ξ. The psd $n(\vec{x}, t; \xi)$, where $\vec{x}$ denotes the spatial coordinates and t is the temporal coordinate, satisfies the General Dynamic Equation (GDE) (Friedlander, 2000)

$$\frac{\partial n}{\partial t} + \nabla \cdot n\vec{u} = \left[\frac{\partial n}{\partial t}\right]_{\text{nuc}} + \left[\frac{\partial n}{\partial t}\right]_{\text{cond}} + \left[\frac{\partial n}{\partial t}\right]_{\text{coag}} \tag{2}$$

where the three terms on the right hand denote nucleation, condensation and coagulation. In the GDE, the diffusion term is neglected owing to the large Schmidt number of aerosol particles. Nucleation is modeled by the classic Becker-Döring theory. Condensation and coagulation are usually modeled differently in different Knudsen number regimes, which are defined according to the particle size compared to the gas mean free path, i.e., free molecular and continuum regimes. The harmonic mean of the models in the two regimes are used. Details of the physical models can be found in Friedlander (2000); Zhou *et al.* (2012).

Instead of directly solving the psd from Eq. (2), only a few moments (four moments in this simulation) are solved in the QMOM, which is much more economic computationally than the former and is able to capture the main characteristics of the aerosol statistics. The kth ($k = 0, 1, 2, \ldots$) order moment is defined as

$$M_k = \int_0^\infty n(\xi)\xi^k \,d\xi \tag{3}$$

Therefore, M_0 is the particle number density $(1/\text{m}^3)$, M_1 the diameter "density" (m/m^3), πM_2 the surface area "density" (m^2/m^3), and $\frac{\pi}{6}M_3$ the volume fraction (m^3/m^3), etc. The dynamic equations for the moments set are obtained by applying the moment transformation to the GDE, i.e., multiplying by ξ^k and integrating over the particle size space. The details of the QMOM can be found in Refs. (McGraw, 1997; Marchisio & Fox, 2005).

Lagrangian particles scheme

The Lagrangian particles scheme circumvents the moments realizability problems encountered in conventional advection schemes. Besides, the low numerical diffusion property of the Lagrangian particles scheme makes it easy to track the sharp front of the motion of aerosol particles, and makes it an ideal tool to investigate the differential diffusion of aerosol particles and the gas. Differential diffusion of soot in combustion flames has received many investigations (Lignell *et al.*, 2007; Bisetti *et al.*, 2012), however, to the best of the authors knowledge, it has never been investigated for aerosol particles in non-combustion environment.

In the Lagrangian particles [1] scheme, the movement of a large number of Lagrangian particles is tracked. Physical variables of interest (aerosol moments here) are tied to these Lagrangian particles and evolve along the Lagrangian trajectories. Under this frame work, the conservation equations [2] are separated to two parts, convection and unsteady evolution. The convection is dealt with through an average scheme over particles, and the unsteady evolution of the variables along a trajectory is obtained by solving the corresponding control equations, which are only ordinary differential equations. For the details of the scheme, refer to Attili & Bisetti (2013).

---

[1] Except where explicitly stated, particles in this subsection refer to mathematical objects, rather than physical aerosol particles as discussed elsewhere in this paper.
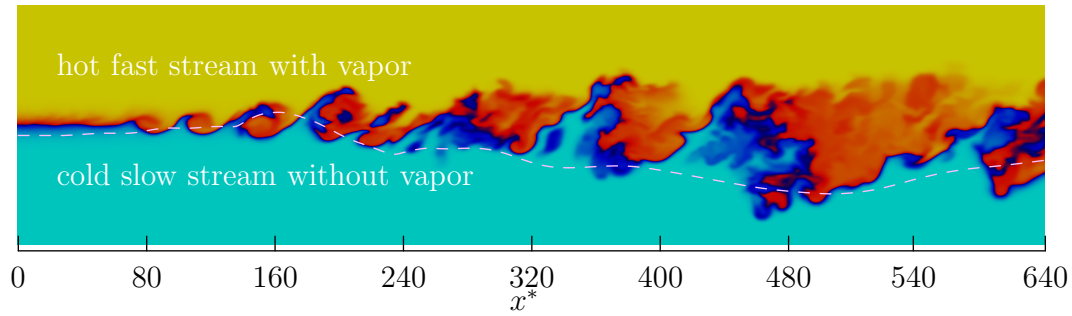
[2] Aerosol diffusion is neglected.

Figure 1. Schematic view of the flow, with a snapshot of the temperature (2D slice, clipped in the cross direction). The dashed line shows a selected Lagrangian particle trajectory. It is worth pointing out that the trajectory is obtained by tracking a fluid parcel with time, while the snapshot is taken at a single time instant.
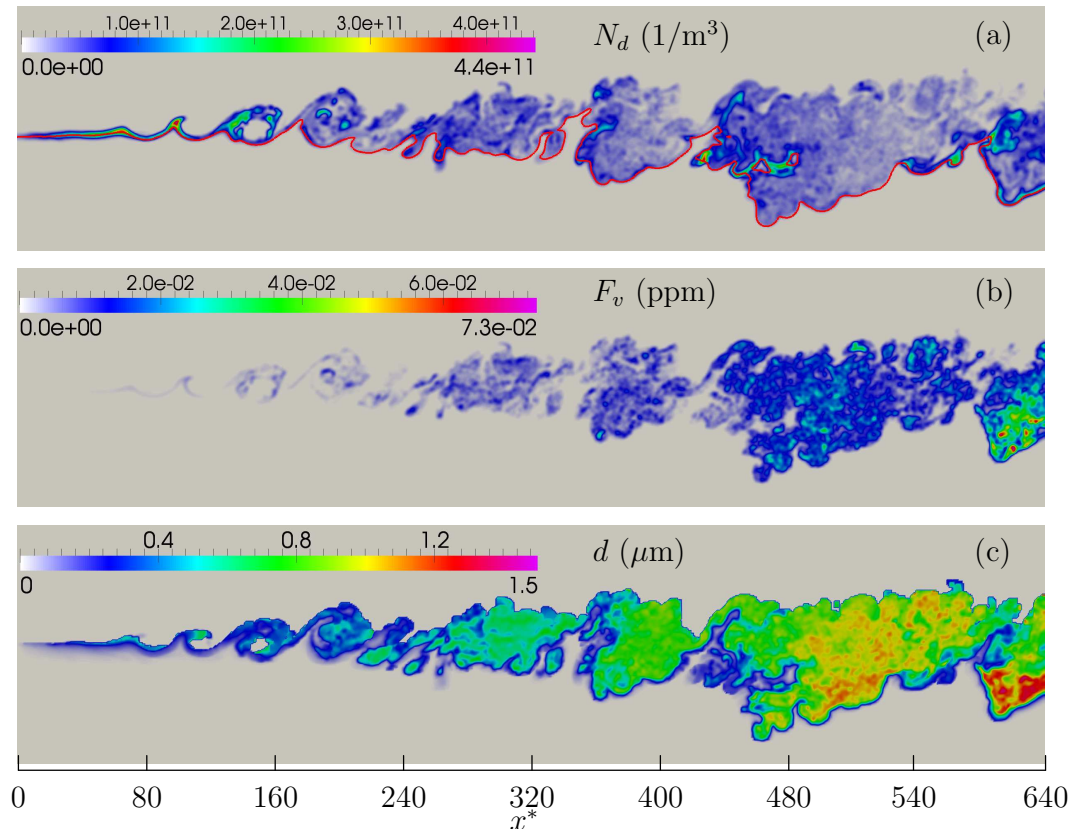

Figure 2. Snapshots of the instantaneous fields. (a) number density (The continuous red curve is the temperature iso-contour corresponding to the maximum nucleation rate.), (b) volume fraction, (c) count mean diameter (cmd).

RESULTS AND DISCUSSION
Aerosol evolution overview

Particle number density and volume fraction are the most important statistical quantities describing aerosol particles. The count mean diameter (cmd), $d = M_1/M_0$, although not directly solved in the QMOM, is also very useful. Figure 2 shows snapshots of the instantaneous fields of number density, volume fraction, and cmd. For the number density, high value is found in the laminar region near the inlet, which is due to high nucleation rate and weak mixing there. In turbulent region, high number density is typically found in the outer region of a vortex. Although nucleation takes place at relatively low temperature [see the red curve Fig. 2(a)], it is possible to find high number density regions on the hot, rich vapor side, when a cold air parcel is convected to the hot side. Very differently from the number density, the volume fraction increases along the streamwise

direction, because of the increase of the aerosol residence time. High volume fraction typically appears in the inner region of a vortex, because condensation growth has the highest rate at intermediate temperature (around 370 K under the conditions of this simulation). Typically, particles on the hot, rich vapor side are larger than those on the cold, lean vapor side. A persistent narrow layer of nanometer-sized particles is found on the cold, lean vapor side.

Spatial statistics of aerosol

The mean cross-stream profiles of the number density, volume fraction and cmd at six streamwise locations are shown in Fig. 3. The normalized crosswise coordinate is defined as $y^+ = y/\delta_{x^*}$, where δ_{x^*} is the momentum thickness of the mixing layer.

The peak mean number densities in the laminar and

transition regions ($x^* = 42$ and $x^* = 83$) is much higher than those in the turbulence region, where the flow fluctuations are much larger and the mean over high and low number densities renders a smaller value than in the laminar region. While in the turbulent region (from $x^* = 249$ to $x^* = 581$), the mean peak number density increases along the streamwise direction. That is because nucleation keeps generating particles along the streamwise direction.

The peak mean volume fraction increases along the streamwise direction, in contrast to the number density. The increase of the volume fraction is mainly due to condensation. Nucleation has a negligible direct contribution to the volume fraction, since nucleated particles are very small despite the huge number. The increasing rate of the volume fraction along the streamwise direction is super-linear, due to higher number and larger surface of particles for vapor to condense on.

Due to condensation growth, particles become larger when traveling downstream [Fig. 3(c)]. However, at $x^* = 42$, the mean cmd profile has an abnormally high peak value around $y^+ = 0.4$. On one hand, particles grow very fast due to condensation. On the other hand, the crosswise convection of particles is very weak in the laminar region. Huge number of nanoparticles nucleated in the cool vapor side (negative y^+) are not transported to the hot vapor side. Hence, the cmd shows an abnormal high peak at the laminar region. After then, the cmd is found to decrease from $x^* = 42$ to $x^* = 83$, which is due to stronger mixing of large and small particles.

Although the mean statistics are the most easily accessible quantities in turbulence measurements, yet there is no experimental data available for aerosol evolution in a mixing layer. However, based on the experimental results of DBP aerosol in a turbulent round jet, Lesniewski & Friedlander (1998) concluded that nucleation mostly takes place in the shear layer region of the jet (a distance of five times of the orifice diameter from the inlet). Due the sensitivity of the nucleation rate on the temperature and vapor concentration, and the uncertainty in the classic nucleation theory, it is very difficult to compare numerical simulations with experiments with regards to the aerosol number density (Veroli & Rigopoulos, 2011). Despite the difficulties, the simulation results here qualitatively agree with the experiment measurements (Lesniewski & Friedlander, 1998) on many aspects. The mean number densities are of the same order of magnitude $10^{10}(1/m^3)$ at the turbulent region far away from the inlet at the same residence time in the mixing layer here and the round jet (Lesniewski & Friedlander, 1998). The vapor concentration dilutes quickly along the streamwise direction in a round jet, while in the mixing layer the vapor concentration is nearly constant (vapor depletion due to gas-to-particle conversion is not significant here). Nucleation continuously generates particles in the mixing layer here. However, nucleation dies out quickly a few diameters away from the inlet in a jet flow. On another aspect, the measured mean cmd in the turbulent jet is from 0.4 to 0.5 μm. In the simulation here, the mean cmd is from 0.42 ($x^* = 249$) to 0.75μm ($x^* = 581$). As discussed shortly before, aerosol particles traveling downstream undergo higher vapor concentration in the mixing layer than in a round jet when they have the same maximum vapor concentration at the inlet. Therefore, the mean particle size is slightly bigger in the mixing layer.
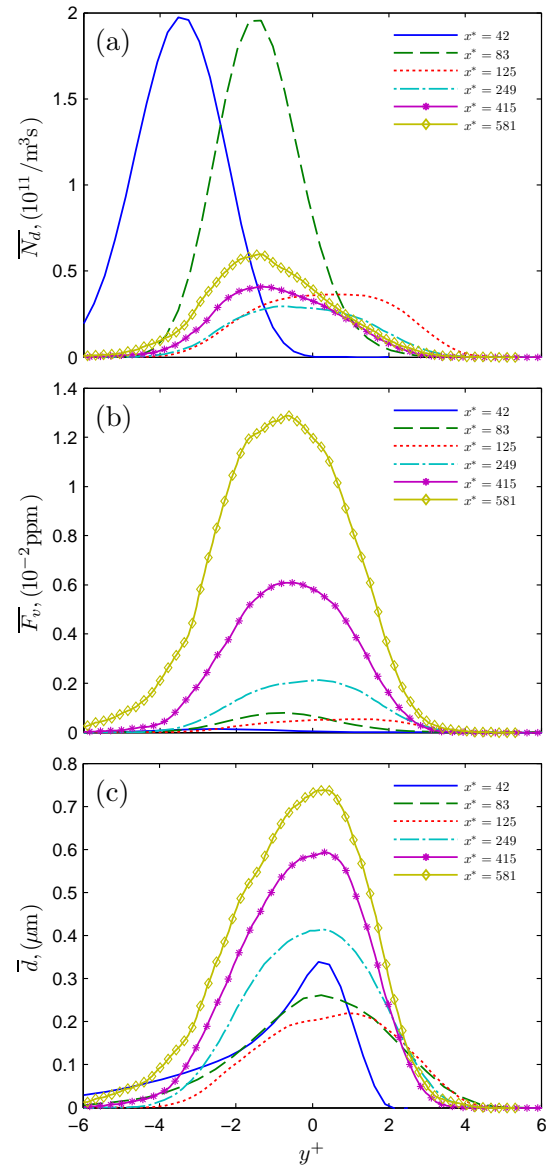

Figure 3. Mean cross profiles. (a) number density, (b) volume fraction, (c) cmd.

Conditional mean profiles of aerosol

The effect of differential diffusion of aerosol particles and the gas can be explained easily the mean conditioned on the mixture fraction, ϕ, which is a passive scalar with value 1 on the hot rich vapor side and 0 on the other side. Figure 4(a) shows the conditional mean number density profiles. At $x^* = 42$, $\widetilde{N_d}$ has a peak around $\phi = 0.17$, which corresponds to the maximum nucleation rate. In fact, nucleation only takes place on the cool vapor side. However, the profiles of $\widetilde{N_d}$ at downstream positions have long tails to the right. This is due to the differential diffusion between diffusive scalars and aerosol particles. The profile at $x^* = 125$ exhibits a peak at $\phi = 0.4$, far away from the peak mixture fraction at other locations. This shows that the big flow fluctuation in the transition region has stronger effect to transport the aerosol particles towards high mixture fraction direction.

Figure 4(b) shows the conditional mean volume fraction. At $x^* = 42$, the profile has a peak at $\phi = 0.2$, very close to the maximum nucleation rate position $\phi = 0.17$. Although nucleation generates large number of particles, yet
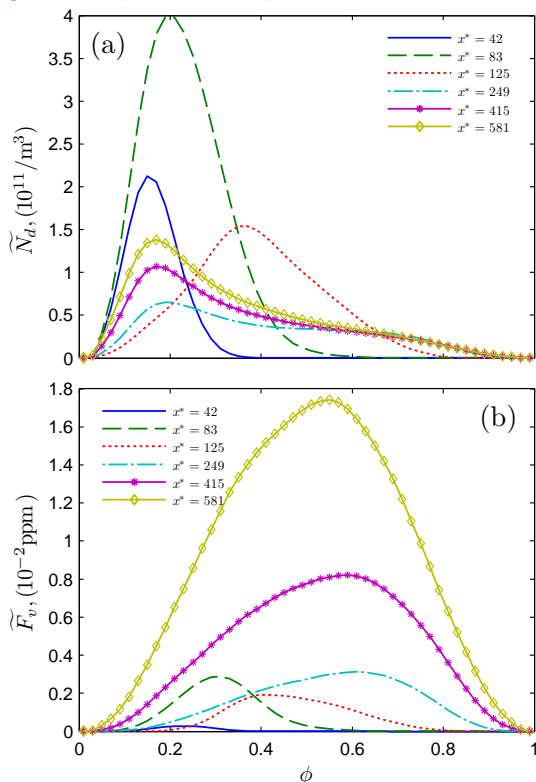
Figure 4.   Conditional mean in the mixture fraction space. (a) number density, (b) volume fraction.

Figure 5.   Temperature and nucleation rate along a trajectory. The gray zone denotes the teperature range at which nucleation mostly take place (The cut-off threshold is 1% of the peak nucleation rate).

its direct contribution to the volume fraction is negligible. In the turbulent region, the peak volume fraction appears at the center region. Close scrutiny shows that at $\phi = 0.7$ the particles have the highest condensation growth rate. The peak volume fraction actually appears in the middle of two interesting regions, i.e., high nucleation rate region to the left and high condensation growth rate region to the right.

Aerosol evolution along a trajectory

During the simulation, the flow and aerosol variables have also been investigated along Lagrangian trajectories. Figure 5 shows the temperature profile along a representative Lagrangian particle trajectory (corresponding to the trajectory in Fig. 1). The corresponding nucleation rate is also shown. Since vapor depletion is negligible in this simulation, the vapor concentration is almost linearly correlated with the temperature. Hence, the nucleation rate is almost completely determined by the temperature. Nucleation mostly takes place in a narrow temperature region (marked with gray block in Fig. 5). Large number of aerosol particles are generated when a fluid parcel passes this active nucleation region (in temperature space).

In order to obtain the aerosol psd, a MC is used to simulate the aerosol evolution. Although coupling MC simulation of aerosol dynamics with computational fluid dynamics is computationally prohibitive, MC can be used to simulate the aerosol evolution along selected trajectories. Figure 6 compares the number densities and volume fractions obtained by the QMOM and the MC (Zhou & Bisetti, 2013) along the selected trajectory. The QMOM and the MC give the same result for the number density. The N_d profile behaves like a staircase, to be almost constant between abrupt jumps, which correspond to the bursts of aerosol particles
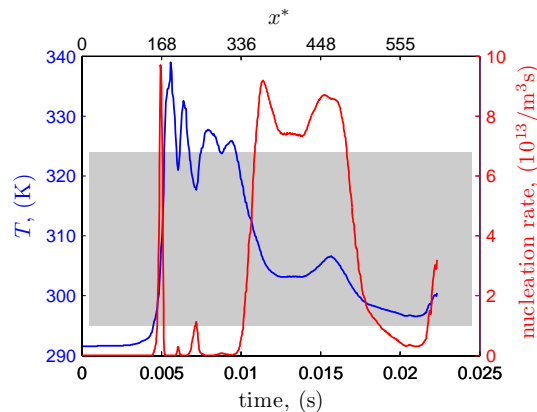
from nucleation. The volume fraction given by the QMOM also agrees with the MC result very well. The volume fraction increases all the way due to condensation. Although the QMOM and the MC agree with each other extremely well here, yet this agreement can not be guaranteed in general. In this simulation, the number density is dominated by the nucleation process, and coagulation is negligible due to the low number density. Nucleation is only dependent on the temperature and vapor concentration, independent of the existing aerosol particles, therefore the same number density profile is observed. On the other hand, condensation growth is mainly in the free molecular regime, which is independent of the particle size. In other words, the evolution of the volume fraction is insensitive to the actual psd. When coagulation is significant and condensation has stronger dependence on particles size, the results from the QMOM and the MC might differ to a greater extent.

One advantage of MC over the QMOM is that MC can provide the psd. Figure 7 shows the psd at the end of the trajectory. The results from 300 and 500 thousand samples are compared to check the stochastic convergence. The psd shows complex multi-modal distribution. The peaks in the psd are closely related to the nucleation rate curve in Fig. 5. The rightmost peak in the psd corresponds to the leftmost spiky peak in the nucleation rate curve, where the nucleated particles have the longest residence time to grow to the largest ones. Particles in the big peak in the psd from 100nm to 400nm are generated in the nucleation burst during 0.01s to 0.018s in Fig. 5. The big trough in the psd corresponds to the dip in the nucleation rate around 0.02s. Particles under a few tens of nanometer in the psd are generated in a narrow time period after 0.02s. The relatively broad distribution of these nanometer-sized particles is due to the fast condensation growth rate for small particles. As this example psd shows, the combination of nucleation and condensation can render very complicate distribution. The distribution may even be discontinuous when nucleation ceases to generate particles for an extensive period of time and the particles still grow due to condensation.

CONCLUSIONS

Nucleation and growth of dibutyl phthalate particles in a turbulent mixing layer has been simulated through the combination of direct numerical simulation for the flow
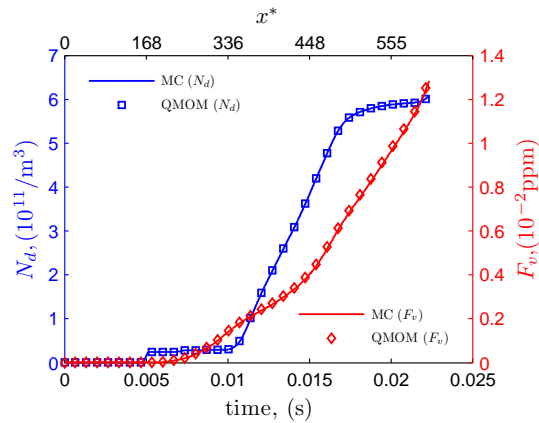
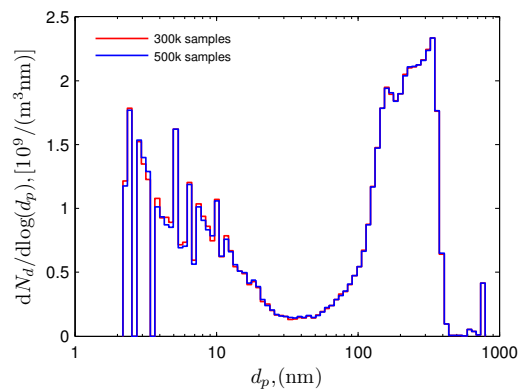Figure 6. Number density and volume fraction along the trajectory.

Figure 7. The psd at the end of the trajectory. The area under the curve is the total particle number density.

field and the quadrature method of moments for aerosol dynamics. A Lagrangian particles scheme is used to transport the moments of the particle size density function. The simulation results show that the highest nucleation rate region is located on the cold, lean vapor region, while particles experience a high growth rate on the hot, rich vapor region. The differential diffusion of aerosol particles and the gas is investigated. Small nucleated particles tend to drift towards the hot, rich vapor region, while bigger particles from condensation growth drift towards the cold, lean vapor region. Due to this movement, the particle volume fraction peaks in the middle region of the mixture fraction space. A Monte Carlo simulation of aerosol dynamics has been performed along a selected trajectory. The particle size distribution exhibits complex modality due to the synergistic effect of nucleation and coagulation.

REFERENCES

Attili, A. & Bisetti, F. 2012 Statistics and scaling of turbulence in a spatially developing mixing layer at Re$_\lambda$ = 250. *Physics of Fluids* **24**, 035109.

Attili, A. & Bisetti, F. 2013 Application of a robust and efficient lagrangian particle scheme for the evolution of soot statistical moments in turbulent flames. *Computers & Fluids* (under review).

Bisetti, F., Blanquart, G., Mueller, M. E. & Pitsch, H. 2012 On the formation and earlyevolution of soot in turbulent nonpremixed flames. *Combustion and Flame* **159**, 317–335.

Desjardins, O., Blanquart, G., Balarac, G. & Pitsch, H. 2008 High order conservative finite difference scheme for variable density low Mach number turbulent flows. *Journal of Computational Physics* **227** (15), 7125–7159.

Falgout, R., Jones, J. & Yang, U. 2006 The design and implementation of hypre, a library of parallel high performance preconditioners. In *Numerical Solution of Partial Differential Equations on Parallel Computers* (ed. A. M. Bruaset & A. Tveito), pp. 267–294. Springer.

Friedlander, S. K. 2000 *Smoke, Dust, and Haze: Fundamentals of Aerosol Dynamics*, 2nd edn. New York: Oxford University Press.

Garmory, A. & Mastorakos, E. 2008 Aerosol nucleation and growth in a turbulent jet using the Stochastic Fields method. *Chemical Engineering Science* **63** (16), 4079–4089.

Kim, J. & Moin, P. 1985 Application of a fractional-step method to incompressible Navier-Stokes equations. *Journal of Computational Physics* **59** (2), 308–323.

Lesniewski, T. K. & Friedlander, S. K. 1998 Particle nucleation and growth in a free turbulent jet. *Proceedings of the Royal Society of London. Series A* **454**, 2477–2504.

Lignell, D. O., Chen, J. H., Smith, P. J., Lu, T. & Law, C. K. 2007 The effect of flame structure on soot formation and transport in turbulent nonpremixed flames using direct numerical simulation. *Combustion and Flame* **151**, 2–28.

Liu, X.-D., Osher, S. & Chan, T. 1994 Weighted essentially non-oscillatory schemes. *Journal of Computational Physics* **115**, 200–212.

Marchisio, D. L. & Fox, R. O. 2005 Solution of population balance equations using the direct quadrature method of moments. *Journal of Aerosol Science* **36**, 43–73.

Marchisio, D. L., Vigil, R. D. & Fox, R. O. 2003 Quadrature method of moments for agrregation-breakage processes. *Journal of Colloid and Interface Science* **258**, 322–334.

McGraw, R. 1997 Description of aerosol dynamics by the quadrature method of moments. *Aerosol Science and Technology* **27** (2), 255–265.

Ol'shanskii, M. A. & Staroverov, V. M. 2000 On simulation of outflow boundary conditions in finite difference calculations for incompressible fluid. *International Journal for Numerical Methods in Fluids* **33** (4), 499–534.

Veroli, G. Y. D. & Rigopoulos, S. 2011 Modeling of aerosol formation in a turbulent jet with the transported population balance equation-probability density function approach. *Physics of Fluids* **23** (4), 043305.

Zhou, K., Attili, A. & Bisetti, F. 2012 Direct numerical simulation of aerosol growth processes in a turbulent mixing layer. In *Seventh International Conference on Computational Fluid Dynamics (ICCFD7), Big Island, Hawaii, July 9-13*.

Zhou, K. & Bisetti, F. 2013 Operator splitting Monte Carlo: A highly efficient simulator for aerosol dynamics. *Journal of Computational Physics* (in preparation).